Research Article **Open Access**

Joko Sedyono, Homayoun Hadavinia*, Demetrios Venetsanos, and Denis R. Marchant

Enumeration search method for optimisation of stacking sequence of laminated composite plates subjected to buckling

Abstract: Enumeration search method (ESM) checks all possible combinations of design variables in a bottom-up approach until it finds the global optimum solution for the design conditions. In this paper an optimum design of a multilayered laminated plate made of unidirectional fibre reinforced polymer (FRP) composite subject to uniaxial compression is sought. ESM together with classical laminated plate theory (CLPT) has been used to find the lightest laminate for maximizing the buckling load capable of providing structural stability for a set target uniaxial compression load. The choice of the design variables is limited to 4 possible fibres orientation angles (0,90,-45,+45) and the sequence of the laminate, making the problem an integer programming. Experimental and finite element analyses were used to verify the optimum solution. It has been shown that the exhaustive enumeration search method is a powerful tool for finding the global optimum design.

Keywords: optimisation; laminated plate; exhaustive search; plate buckling

DOI 10.1515/eng-2015-0025
Received August 13, 2014; accepted March 17, 2015

1 Introduction

The use of fibre reinforced composite materials originated from their application in weight- critical military aerospace structures, and then more recently has expanded in areas such as commercial aircraft, automobiles, robotic arms, wind turbine blades and various architectural applications.

In contrast to metallic materials, structural analysis of fibre reinforced polymer (FRP) laminated composite plates is more complicated due to the anisotropy of each layer, and as a result, the design of laminated FRP plates includes additional complexity. An efficient composite structural design that meets all the requirements for a specific application can be achieved not only by sizing the cross-sectional areas and member thicknesses, but also by tailoring of the material properties through selective choice of fibre orientation and stacking sequence of the layers that make up the composite laminate. Therefore, selecting the optimum laminate sequence requires a systematic optimisation approach [1, 2]. In addition, the laminated composite structures are usually thin walled structures and buckling of FRP composite elements such as plates, shells, columns *etc*. whether slender or thin is an important aspect and certainly should be considered carefully at the design stage. In aerospace structures, thin walled members are generally used due to weight considerations; hence, they are prone to buckling under in-plane loads [3, 4]. Unlike beams, where buckling is, typically, very near to ultimate failure, plates may have significant post-buckling ability [5].

In 1995 Fukunaga *et al*. [6] studied optimization of symmetrically laminated plates with simply supported or clamped edges to maximize buckling loads under combined loading. In their analysis they considered the coupling between bending and twisting. The optimal laminate configuration to maximize the buckling loads was obtained using a mathematical programming method where four lamination parameters were used as design variables.

Walker *et al*. [7] used a finite element approach for the optimal stacking sequence design of symmetric laminated composite plates for maximum buckling load subjected to biaxial compression. The effect of optimization on the buckling load was investigated by plotting the buckling load against the design variable. The results show that the difference in the buckling loads of optimal and non-optimal plates could be quite substantial, emphasizing the importance of optimization for fibre composite structures.

Walker [8] studied optimal design of biaxially loaded laminated plates constrained under a combination of free,

***Corresponding Author: Homayoun Hadavinia:** Material Research Centre, Kingston University London, SW15 3DW, UK, E-mail: h.hadavinia@kingston.ac.uk
Joko Sedyono: Material Research Centre, Kingston University London, SW15 3DW, UK
Joko Sedyono: Universitas Muhammadiyah Surakarta Indonesia
Demetrios Venetsanos, Denis R. Marchant: Material Research Centre, Kingston University London, SW15 3DW, UK

simply supported and clamped edge boundary conditions for a maximum weighted combination of buckling load and resonance frequency. In a further study Walker [9] also presented optimal designs of symmetrically laminated rectangular plates with different stiffener arrangements. The plate designs are optimised with the objective of maximising the biaxial buckling load with the ply fibre orientation as the design variable. During the optimisation procedure, the capability of each laminate design is determined using the finite element method. The plates were subject to a combination of simply supported, clamped and free boundary conditions.

Sciuva *et al.* [10] performed optimization of laminated and sandwich plates with respect to buckling load and laminate thickness, using different sets of constraints such as the fundamental frequency, the maximum deflection under transverse uniform distributed load, the mass and the buckling load. The genetic and simulated annealing algorithms were employed together with two plate models. Adali *et al.* [11] presented optimal design of composite laminates under buckling load uncertainty. The laminates were subjected to biaxial compressive loads and the buckling load was maximized under worst-case scenario in plane loading.

Kogiso *et al.* [12] carried out the reliability-based design approach to the composite laminated plate subjected to buckling. The reliability is evaluated by modelling the plate as a series system consisting of eigenmodes, considering the asymmetry of laminates due to the random variation of the material constants and the orientation angles. It is shown that the reliability-based design is different from the deterministic optimum design for almost all the load cases. Especially, the ply angle difference between the surface and the mid-plane layers of the reliability-based design is larger than that of the deterministic one.

Latalski [13] considered ply thicknesses perturbations in the laminate plate optimum design results in a different ply stacking sequence when compared to the solutions of the nominal design problem. This justified the incorporation of thicknesses perturbations in the optimization design algorithm. It is shown that this approach is necessary for mid- Ny/Nx load ratios, but has no practical importance for very low or very high load ratios since the nominal and robust designs in these specific cases are identical.

Lindgaard and Lund [14] presented nonlinear buckling fibre angle optimization of laminated composite structures. The approach accounts for the geometrically nonlinear behaviour of the structure by utilizing response analysis up until the critical point. They obtained the sensitivity information by an estimated critical load factor at a precritical state. In the optimization formulation, the risk of "mode switching" is avoided by including the lowest buckling factors. The presented optimization formulation is compared to the traditional linear buckling formulation and two numerical examples, including a large laminated composite wind turbine main spar, were studied.

Hemmatian *et al.* [15] applied Ant Colony Optimisation (ACO) for the multi-objective optimization of hybrid laminates for obtaining minimum weight and cost. The hybrid laminate is made of glass fibre reinforced polymer (GFRP) and carbon fibre reinforced polymer (CFRP) plies using a modified variation of ACO so called the Elitist Ant System (EAS) in order to make the trade-off between the cost and weight as the objective functions. The first natural frequency was considered as a constraint. The results obtained using the EAS method including the Pareto set, optimum stacking sequences, and the number of plies made of either glass or graphite fibres were compared with those reported in literature using the Genetic Algorithm (GA) and Ant Colony System (ACS).

Kim *et al.* [16] optimized the stacking sequence of the composite layer using a micro-genetic algorithm and its effects on the performances of static/buckling load capability and stiffness of an automotive lower arm. They performed the design optimization with the linear perturbation eigenvalue analysis, targeting a 50% weight reduction of a conventional steel arm.

Ferreira *et al.* [17] used hierarchical optimization for laminated composite structures. They considered simultaneously the design of structure and material at macroscopic and microscopic levels. At the macroscopic level, they considered fibre orientations and fibre volume fraction of unidirectional composite layers. At the microscopic level they considered the size of cross-sectional area and the shape of the reinforcement fibres. Both levels are coupled by a resource constraint and exchange derivatives in a mathematically consistent manner. The objective was to minimize compliance under a total fibre volume fraction constraint. The plies orientations are chosen using the Discrete Material Optimization (DMO) approach. The results show that the optimization procedure permits to increase structural stiffness when material microstructural characteristics are optimised. For a detail review of optimal design of composite structure refer to Ganguli [18].

Enumeration search method (ESM) is an exhaustive search strategy that checks all possible combinations of design variables in a bottom-up approach until it finds the optimum solution for the design conditions. Although cumbersome, this technique was used to find the lightest composite laminate during the 1970s [19, 20].

Legland and Beaugrand [21] used ESM exhaustive search method to determine the formal definition of the

geodesic diameter of natural fibre for characteristic of morphometric features and particle clustering. Park [22] obtained the optimal design angles and presented them in a graphical form as functions of the loading conditions. The results can be directly used by laminate designers for making a choice of composites with optimal performance. Weaver [23] built a database that stores appropriate properties of all permutations of lay- up angles for a laminate. He came up with selection charts in which each class of laminates was displayed within an elliptical contour. These charts can be used to identify a small subset of potential laminates that might be investigated in more details. ESM has also been applied in other fields such as in computer science [24, 25] and electronic rewiring [26]. In none of the previous works was the use of a systematic approach for choosing the stacking sequence using ESM reported, charts being used instead. ESM optimisation technique will be used in the present work.

Other solution methods for integer/discrete programming problems include branch and bound method, cutting plane, heuristic methods, *etc*. The branch and bound method is based on the observation that the enumeration of integer solutions has a tree structure. The name of the method comes from the branching that happens when a node is selected for further growth and the next generation of children of that node is created. The bounding comes in when the bound on the best value attained by growing a node is estimated. We hope that in the end we will have grown only a very small fraction of the full enumeration tree [27]. The cutting-plane method is an umbrella term for optimization methods which iteratively refine a feasible set or objective function by means of linear inequalities, termed cuts. Such procedures are popularly used to find integer solutions to mixed integer linear programming (MILP) problems, as well as to solve general, not necessarily differentiable convex optimization problems. The use of cutting planes to solve MILP was introduced by Gomory and Chvátal [28, 29].

In this study, the minimum weight of a symmetric unidirectional FRP composite plate is sought when the plate is subjected to a uniaxial compressive loading. ESM together with classical laminated plate theory (CLPT) has been used to find the lightest laminate for maximizing the buckling load capable of providing structural stability for a set target uniaxial compression load. The choice of the design variables is limited to 4 possible fibres orientation angles (0,90,-45,+45) and the sequence of the laminate, making the problem an integer programming. The optimum stacking sequence is the output of the computer programme. Experimental and finite element analyses were used to verify the optimum solution.

2 Calculating critical buckling load for FRP laminated plates

The load-displacement behaviour of a plate subjected to compressive in-plane load P, causing an out of plane displacement w measured typically at one of the crests of a buckle is shown in Figure 1 (following [30]). The Euler elastic critical buckling load for a linearized idealisation, P_C, is when the plate will suddenly loose in-plane stiffness (A-C). This point is called the bifurcation point as the load path branches into two possible equilibrium paths. The other possible solution path, though unstable, is A-B. If large displacement and large rotation geometric nonlinearity are considered in the analysis for the perfect plate under in-plane loading, path A-D (shown in Figure 1) will be predicted where the stiffness is increasing as the load increases [31, 32]. The plate behaviour after bifurcation is called the post-buckling region. This region is important as it shows the plate is capable of carrying load far beyond the critical load. However, in this region the stiffness is significantly reduced so the behaviour should be known precisely.

In the buckling analysis, some assumptions are made such as an initially perfect flat plate and material behaviour that does not precisely describe reality. These assumptions put limitations on the theoretical results. All materials to some extent are imperfect and may contain flaws of varying magnitudes. For example, a manufactured FRP composite plate has an initial curvature, nonuniform resin rich areas between the plies and probably residual stresses from uneven cooling during curing of laminates or some machining damage may exist in the plate. However, in our analysis the flat plate assumed to be perfect noting that in the buckling behaviour of structures, the material and geometric imperfections have been proven experimentally to be detrimental.

When the assumptions are found to be an ideal description of the actual behaviour of the flat plates, the question arises how these initial imperfections affect the plate behaviour before, as well as after, the bifurcation point. Figure 1 shows the difference in behaviour of a flat plate when the plate imperfections are considered. Considering Figure 1, two conclusions concerning how the imperfection influence the plate behaviour may be drawn. Firstly, buckling of a flat plate with inherent imperfections is gradual and it is very difficult to specify exactly when critical load has been reached. Hence, there will be some discrepancies between theoretical and experimental buckling load. Secondly, the plate may continue to carry load after the bifurcation point. Thus, the critical load is a con-

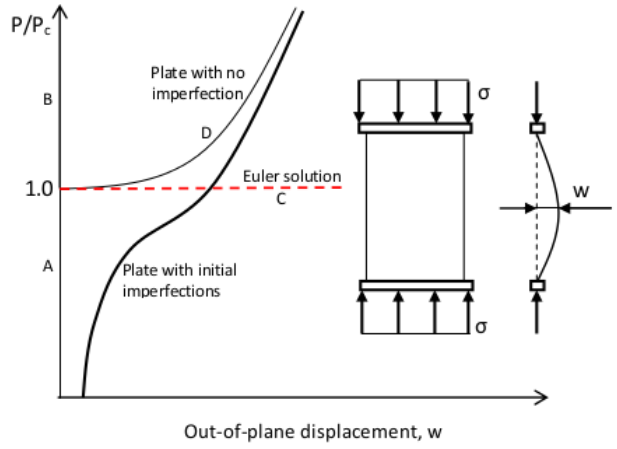

Figure 1: The influence of initial plate imperfections on buckling behaviour of a plate (following [30]).

servative estimate of the ultimate buckling resistance of the plate in question. As a result, the selection of critical buckling load extracted from experimental load versus the out-of-plane displacement diagram is not well defined. In this work the critical buckling load was extracted at the intersection of tangents to the postbuckling section and initial stiffness line of the diagram as will be discussed later.

2.1 Critical buckling load from analytical solution

In the ESM optimisation the analysis of flat plate buckling is based on CLPT [5, 33]. According to CLPT, the components of reduced stiffness matrix for each ply are:

$$Q_{11} = \frac{E_1}{1-\nu_{12}\nu_{21}},\ Q_{22} = \frac{E_2}{1-\nu_{12}\nu_{21}},$$
$$Q_{12} = \frac{\nu_{12}E_2}{1-\nu_{12}\nu_{21}} = \frac{\nu_{21}E_1}{1-\nu_{12}\nu_{21}},\ Q_{66} = G_{12}, \tag{1}$$

where E_1, and E_2 are modulus of elasticity in fibre and transverse to fibre directions, G_{12} is shear modulus in 12 plane and ν_{12}, ν_{21} are Poisson's ratios. The components of transformed reduced stiffness matrix in the global coordinate system are:

$$\overline{Q}_{11} = c^4Q_{11} + s^4Q_{22} + 2c^2s^2Q_{12} + 4c^2s^2Q_{66}$$

$$\overline{Q}_{22} = s^4Q_{11} + c^4Q_{22} + 2c^2s^2Q_{12} + 4c^2s^2Q_{66}$$

$$\overline{Q}_{12} = c^2s^2Q_{11} + c^2s^2Q_{22} + \left(c^4+s^4\right)Q_{12} - 4c^2s^2Q_{66}$$

$$\overline{Q}_{66} = c^2s^2Q_{11} + c^2s^2Q_{22} - 2c^2s^2Q_{12} + \left(c^2-s^2\right)Q_{66}$$

$$\overline{Q}_{16} = c^3sQ_{11} - cs^3Q_{22} + \left(cs^3 - c^3s\right)Q_{12} + 2\left(cs^3 - c^3s\right)Q_{66}$$

$$\overline{Q}_{26} = cs^3Q_{11} - c^3sQ_{22} + \left(c^3s - cs^3\right)Q_{12} + 2\left(c^3s - cs^3\right)Q_{66}, \tag{2}$$

where $c = \cos\theta$ and $s = \sin\theta$. The extensional (A), coupling (B), and bending (D) stiffness matrices are:

$$A_{ij} = \sum_{k=1}^{nl}[\overline{Q}_{ij}]_k(z_k - z_{k-1}), \tag{3}$$

$$B_{ij} = \frac{1}{2}\sum_{k=1}^{nl}[\overline{Q}_{ij}]_k\left(z_k^2 - z_{k-1}^2\right), \tag{4}$$

$$D_{ij} = \frac{1}{3}\sum_{k=1}^{nl}[\overline{Q}_{ij}]_k\left(z_k^3 - z_{k-1}^3\right). \tag{5}$$

Note that for symmetric laminates [B] matrix is zero.

For large deflection of an especially orthotropic symmetric laminated plate where $A_{16} = A_{26} = 0$, $D_{16} = D_{26} = 0$ and $B_{ij} = 0$, the first von Karman equation becomes:

$$D_{11}\frac{\partial^4 w}{\partial x^4} + 2\left(D_{12}+2D_{66}\right)\frac{\partial^4 w}{\partial x^2\partial y^2} + D_{22}\frac{\partial^4 w}{\partial y^4} = N_x\frac{\partial^2 w}{\partial x^2} + 2N_{xy}\frac{\partial^2 w}{\partial x\partial y} + N_y\frac{\partial^2 w}{\partial y^2} - p_x\frac{\partial w}{\partial x} - p_y\frac{\partial w}{\partial y} - p_z, \tag{6}$$

where w is out-of-plane deflection and p_x, p_y and p_z are distributed loads (force/area). For a plate under biaxial loading and $N_{xy} = p_x = p_y = p_z = 0$, and Equation (6) reduces to:

$$D_{11}\frac{\partial^4 w}{\partial x^4} + 2\left(D_{12}+2D_{66}\right)\frac{\partial^4 w}{\partial x^2\partial y^2} + D_{22}\frac{\partial^4 w}{\partial y^4} = N_x\frac{\partial^2 w}{\partial x^2} + N_y\frac{\partial^2 w}{\partial y^2}. \tag{7}$$

The solution of w for a plate with simply supported edges (SSSS) is:

$$w = \sum\sum A_{mn}\sin\frac{m\pi x}{a}\sin\frac{n\pi y}{b}. \tag{8}$$

Substituting w from Equation (8) in Equation (7) and if the plate aspect ratio defined as $R = a/b$ then

$$\pi^2 A_{mn}\left[D_{11}m^4 + 2\left(D_{12}+2D_{66}\right)m^2n^2R^2 + D_{22}n^4R^4\right] = -A_{mn}a^2\left[N_xm^2 + N_yn^2R^2\right]. \tag{9}$$

Defining $k = N_y/N_x$ and $N_x = -N_C$ then from Equation (9) results

$$N_C = \frac{\pi^2\left[D_{11}m^4 + 2\left(D_{12}+2D_{66}\right)m^2n^2R^2 + D_{22}n^4R^4\right]}{a^2\left(m^2 + kn^2R^2\right)}. \tag{10}$$

For a plate under uniaxial loading $N_y = 0$ thus $k = 0$; and for SSSS boundary condition Equation (10) simplifies to:

$$N_C = \frac{\pi^2 \left[D_{11}m^4 + 2\left(D_{12} + 2D_{66}\right)m^2n^2R^2 + D_{22}n^4R^4\right]}{a^2m^2}. \tag{11}$$

For a plate with clamped-simply supported-clamped-simply supported (CSCS) boundary conditions subjected to uniaxial loading the solution to Equation (7) becomes

$$N_C = \frac{\pi^2}{b^2}\sqrt{D_{11}D_{22}}(K), \tag{12}$$

where N_C is the critical buckling load, b is the width of the specimen, and K is

$$K = \begin{cases} \frac{4}{\lambda^2} + \frac{2\left(D_{12} + 2D_{66}\right)}{\sqrt{D_{11}D_{22}}} + \frac{3}{4}\lambda^2; \\ \quad 0 < \lambda < 1.662 \\ \\ \frac{m^4 + 8m^2 + 1}{\lambda^2(m+1)} + \frac{2\left(D_{12} + 2D_{66}\right)}{\sqrt{D_{11}D_{22}}} + \frac{\lambda^2}{m^2+1}; \\ \quad \lambda > 1.662. \end{cases} \tag{13}$$

In above $\lambda = \frac{a}{b}\left(\frac{D_{22}}{D_{11}}\right)^{1/4}$ and m is an integer number which represents the number of half- wave in load wise direction and a is the length of the plate in the direction of loading.

2.2 Critical buckling load from finite element eigen solution

Finite element modelling was used to obtain the critical buckling load using ANSYS software. The linear buckling analysis in ANSYS finite elements software is performed in two steps. The first step is a linear static analysis of the structure to determine the stresses for a given reference set of loads. Subsequently in the second step an eigenvalue analysis given in the Equation (14) is solved which provides the results in terms of load factors (eigenvalues) and mode shapes (eigenvectors). This equation takes into consideration the prebuckling stress effect matrix [S] calculated in the first step.

$$\left([K] + \lambda_i[S]\right)\{\Psi_i\} = \{0\}. \tag{14}$$

In above $[K]$ is stiffness matrix, $[S]$ is initial stress stiffness matrix, λ_i is the i^{th} eigenvalue (used to multiply the loads which generated $[S]$) and $\{\Psi_i\}$ is the i^{th} eigenvector of displacements. The 'Block Lanczos' method in ANSYS was used to extract the eigenvalues resulting from Equation (14). The eigenvalues obtained from the buckling analysis are factors by which the initially applied force is multiplied. As a result, the critical buckling load is calculated from to Equation (15).

$$P_{cr} = \lambda_{min}PA, \tag{15}$$

where λ_{min} is the minimum eigenvalue, A is the total area on which pressure is applied, and P is the initially applied pressure. By applying a unit pressure ($P = 1$) in Equation (15), the critical buckling load will be as follow

$$P_{cr} = \lambda_{min}A. \tag{16}$$

In all the FEA models SHELL281 elements were used. A unit pressure is applied at the loading edge and the first eigenvalue is the critical buckling load.

3 Optimisation problem

The stacking sequence for a glass fibre reinforced composite flat plate with CSCS boundary conditions with dimensions of 150 mm long; 80 mm wide is to be selected to stand a minimum target buckling load of 200 N/mm with the minimum thickness. The plate is made from symmetric unidirectional plies (UD) with ply nominal thickness of 0.29 mm. This is the benchmark solution of the integer programming problem in composites as the choice of the design variables due to manufacturing constraints is limited to four possible fibres orientation angles (0,90,-45,+45). Any ply angle can be repeatedly used in the stacking sequence.

3.1 Optimisation Formulation

The objective function of the optimisation can be stated as

$$\min \sum \text{weight} = \min \sum \text{number of plies}. \tag{17}$$

Subject to:

$$\frac{N_C}{N_t} \geq 1, \tag{18}$$

where N_C is critical buckling load and N_t is the target applied compressive load. The design variables are the fibre orientation and stacking sequence. The constraint is selection from four possible fibre orientations angles (0,90,-45,+45) for a symmetric laminate. The fibre direction can be repeatedly selected in the stacking sequence.

The optimum solution is sought using the Enumeration Search Method (ESM). ESM is a bottom-up exhaustive search method where all possible combination of plies will be selected and each of the laminates will be tested to check whether the condition in Equation (18) is satisfied or violated. As the method starts from the least possible plies and moving upward until it finds the laminate which satisfies the conditions in Equation (18), the solution will be a global optimum solution.

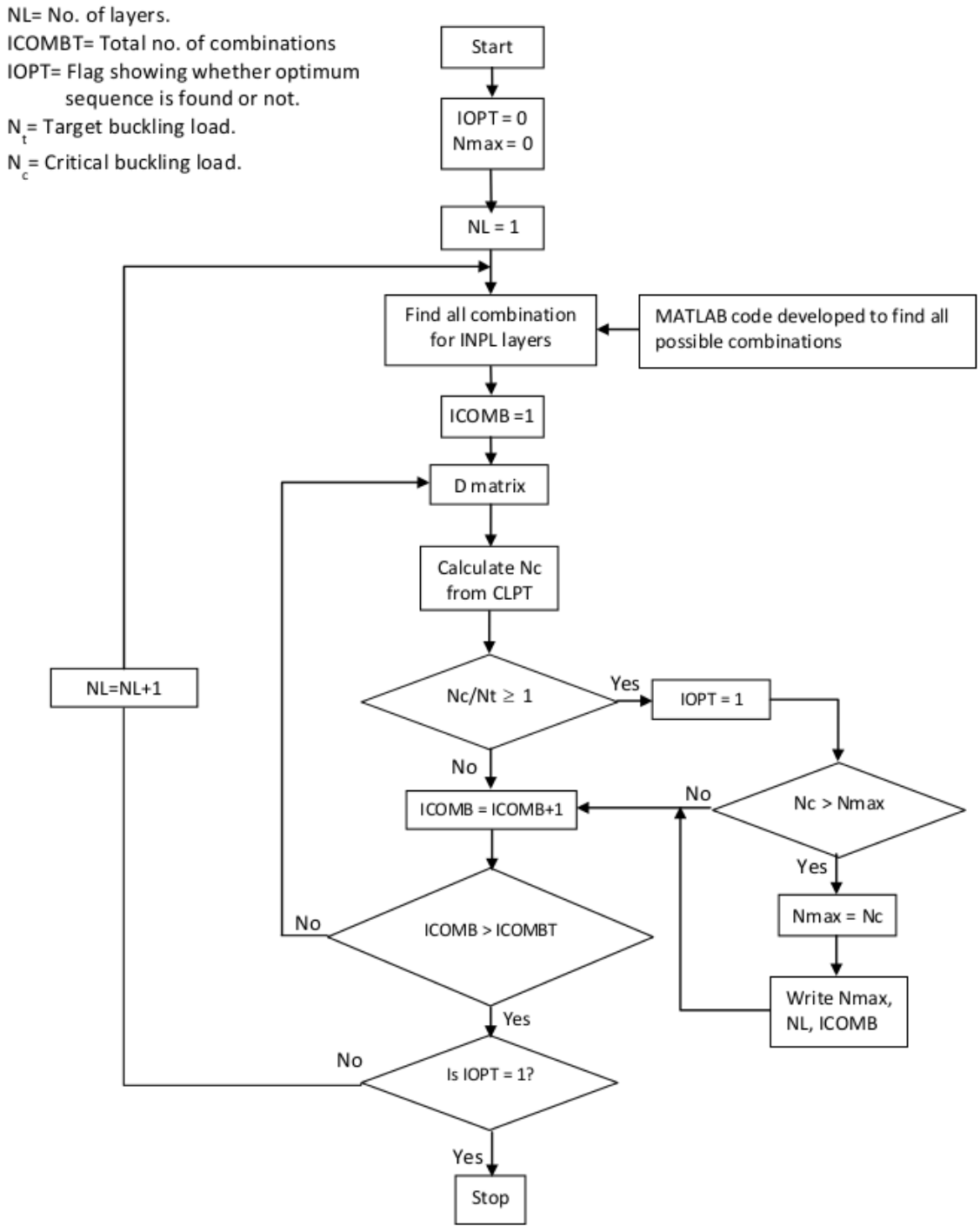

Figure 2: Flow chart of the developed ESM optimisation programming.

Table 1: Mechanical properties of UD GFRP composite material.

E_{11} (GPa)	E_{22} (GPa)	G_{12} (GPa)	ν_{12}	X_t (MPa)	Y_t (MPa)	S (MPa)
37 ± 2	13 ± 1	5 ± 1	0.23 ± 0.01	624 ± 21	71 ± 8	48 ± 1

A programming code in MATLAB has been developed to find all possible stacking sequence combinations for any number of layers from the given ply options. It should be noted that the total number of possible combinations of stacking sequences from p option of layers, and for the symmetric case, can be found from $C_{nl} = p^{nl/2}$, where C_{nl} is total number of combinations and nl is the number of layers. For unsymmetrical lay-up, $C_{nl} = p^{nl}$ can be used. The detail of the ESM programming is described in the flow chart shown in Figure 2.

4 Experimental studies

4.1 Material characterisation

All specimens are fabricated from GFRP prepregs with E722 epoxy matrix supplied by Tencate Advanced Composites, UK. The mechanical properties of the laminate were obtained according to the ASTM D3039 standard[1] for 0° and 90° and ASTM D3518[2] for ±45°. The mechanical properties of the GFRP composite material are summarised in Table 1. X_t is tensile strength in fibre direction, Y_t is tensile strength in normal to fibre direction and S is shear strength. In the FEA studies averaged value of the material properties are used.

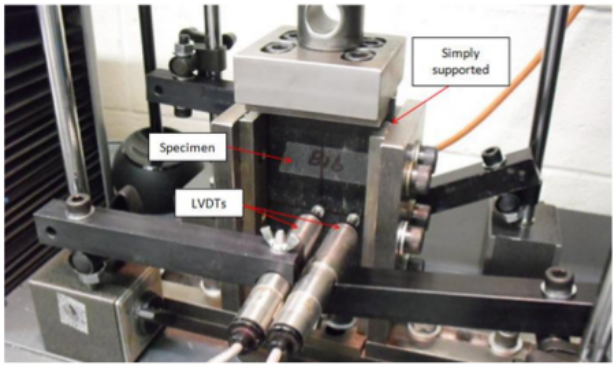

Figure 3: Clamped-simply supported-clamped-simply supported (CSCS) buckling testing rig during operation.

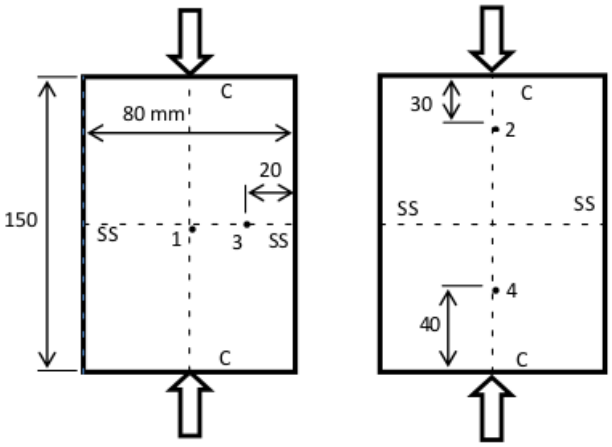

Figure 4: Schematic of buckling test set up showing the location of points where LVDTs are attached.

Table 2: Dimensions of plate specimens in buckling experiments.

Specimen	Length, a (mm)	Width, b (mm)	Plate thickness (mm)
B1a	149.4	80.3	2.33
B1b	150.1	80.1	2.30
B1c	149.2	80.4	2.40
B2a	149.8	80.0	2.30
B2b	150.1	80.0	2.45
B2c	149.1	80.1	2.40
B3a	150.1	80.5	2.30
B3b	150.3	80.0	2.30
B3c	149.6	80.2	2.30
B4a	150.2	80.7	2.40
B4b	150.3	80.6	2.30
B4c	150.2	80.5	2.30

4.2 Buckling tests

The buckling tests were performed according to ASTM D7137 standard[3]. Buckling tests have been done for validation of the ESM results and FEA modelling. The buckling tests are performed using a 50 kN Zwick/Roell universal testing machine. After manufacturing the laminated plates, the test specimens are held in the buckling test fixture during loading (see Figure 3).

The buckling testing rig is placed between the base of the machine and the upper moving head. The machine is stopped when the load drops at failure. The out-of-plane

1 ASTM Specification D3039/D3039M, Standard test method for tensile properties of polymer matrix composites, ASTM International, Conshohocken, PA, 2006.

2 ASTM Specification D3518/3518M, Standard test method for in-plane shear response of polymer matrix composite materials by tensile test of a +-45 laminate, ASTM International, Conshohocken, PA, 2007.

3 ASTM Specification D7137/D7137M, Standard test method for compressive residual strength properties of damaged polymer matrix composite plates, ASTM International, Conshohocken, PA, 2005.

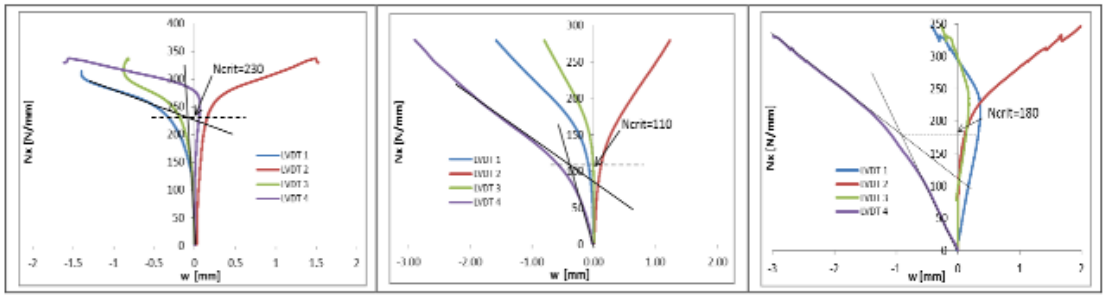

(a) Three B1 specimens test results, sequence $[0/90/0_2]_s$

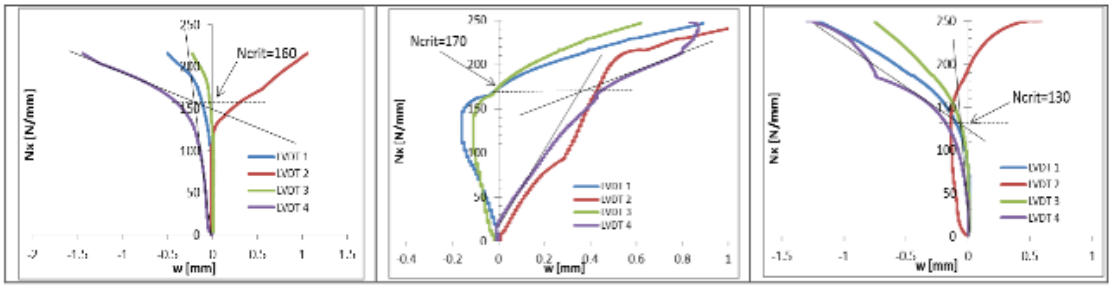

(b) Three B2 specimens test results, sequence $[90/0/\pm45]_s$

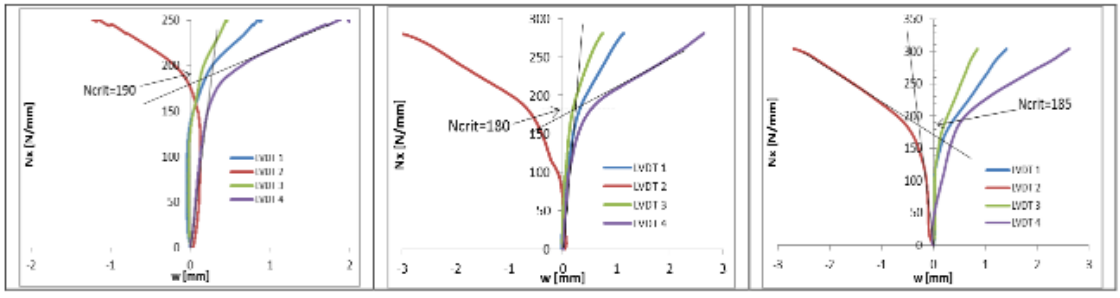

(c) Three B3 specimens test results, sequence $[0_2/90_2]_s$

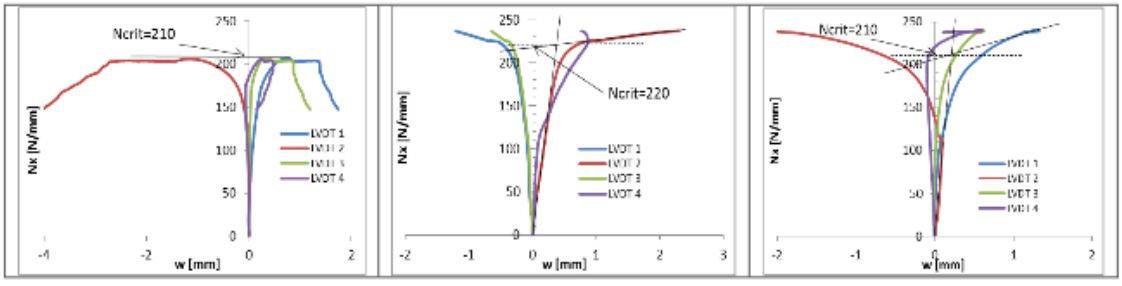

(d) B4 specimens test results, sequence $[\pm45_2]_s$

Figure 5: Load (N/mm) versus out-of-plane displacement (mm) for laminated plates (a) B1, (b) B2, (c) B3 and (d) B4 specimens.

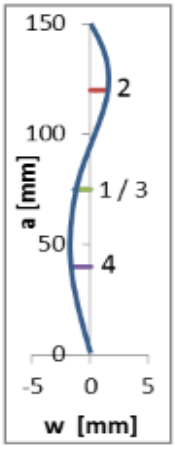

Figure 6: Side view of deformed shape of buckled laminated plate observed in the experiments.

displacements at selected points of the plate are monitored using four linear variable differential transformers (LVDTs) as shown in Figure 3. Figure 4 shows the set-up for the buckling tests. In all the buckling tests the boundary conditions on the plate edges were clamped-simply supported-clamped-simply supported (CSCS).

Three specimens of GFRP flat plates from each of four stacking sequences of $B_1 = [0/90/O_2]_s$, $B_2 = [90/0/\pm 45]_s$, $B_3 = [O_2/9O_2]_s$, and $B_4 = [\pm 45_2]_s$ were manufactured and tested under quasi- static compressive load at a constant cross-head displacement rate of 2 mm/min until failure occurred. Dimensions of plate specimens in buckling experiments are summarised in Table 2. The experimental results of load versus out-of-plane displacement for different buckling tests are shown in Figure 5. The critical buckling load is extracted from the lowest load reading of 4 LVDTs. The critical buckling load was defined at the intersection of the tangents to the post-buckling and initial stiffness as shown in Figure 5 as used by Shukla *et al.* [34]. The extracted experimental critical buckling loads are summarised in Table 5.

The general mode shape of plate buckling obtained from the readings of LVDTs is shown in Figure 6. This figure shows that the mode shape of buckling is antisymmetric with two half waves and it is similar to the first eigen mode solution obtained from finite element simulation. Figure 5 shows that specimen B4 with a stacking sequence of $[\pm 45_2]_s$ *is* the optimum laminate sequence.

5 Optimisation of unidirectional laminated plates

The ESM optimisation is used to determine the stacking sequence for the minimum number of layers from UD plies. All possible solutions for 2, 4, 6 and 8 layers are shown in Figures 7 and 8. The detail of stacking sequences for these cases are summarised in Tables 3 and 4. As shown in Figure 8, the minimum number of layers for which the critical buckling value is equal or bigger than the target buckling load is 8 layers.

Progression of the highest critical buckling load ratio, $\frac{N_C}{N_t}$, for laminates made from UD as the number of plies increases (bottom-up approach) is shown in Figure 9. The result shows that all laminates with 8 layers pass the target buckling load and the optimum solution which is able to carry the highest buckling load is symmetric UD $[\pm 45_2]_s$ plate.

It should be emphasised that the plate buckling analysis is based on the classical laminated plate theory described in Equation (13). However, CLPT is a simplified model which discards factors such as imperfections, non-elastic material behaviour, dynamic effects of the loading, and the fact that the in-plane loading is not applied exactly at the mid-plane. But plates in the real world are not perfectly flat and do not have perfect symmetry. As a result, there are always some differences between experimental and analytical results. In addition, critical buckling loads obtained from FEA eigen buckling solutions are based on geometrically perfect plates. The results of buckling tests and finite element simulations are summarised in Table 5 and shown in Figure 10. These results show that the differences between the FEA modelling, CLPT and experimental results are small; e.g. for specimen number B4, the difference between the critical buckling load from the eigen solution and experiment is -3.2%. Note that in the analytical solution the elastic coupling exists when D_{16} and D_{26} of the bending stiffness matrix [D] are non-zeros. The % error between the FEA results is due to values of D_{16} and D_{26} being non-zeros for plies whose angles are those other than 0° or 90°, thus changing the governing differential equation. Campbell reported that the values of D_{16} and D_{26} become small when a large number of plies are stacked and become insignificant for thicknesses of more than sixteen plies [35].

The mode shape of specimen B4, extracted from FEA analysis is shown in Figure 11. The FEA mode shape matches the experimental results shown in Figure 6 which indicates that the boundary conditions and testing procedure are reliable.

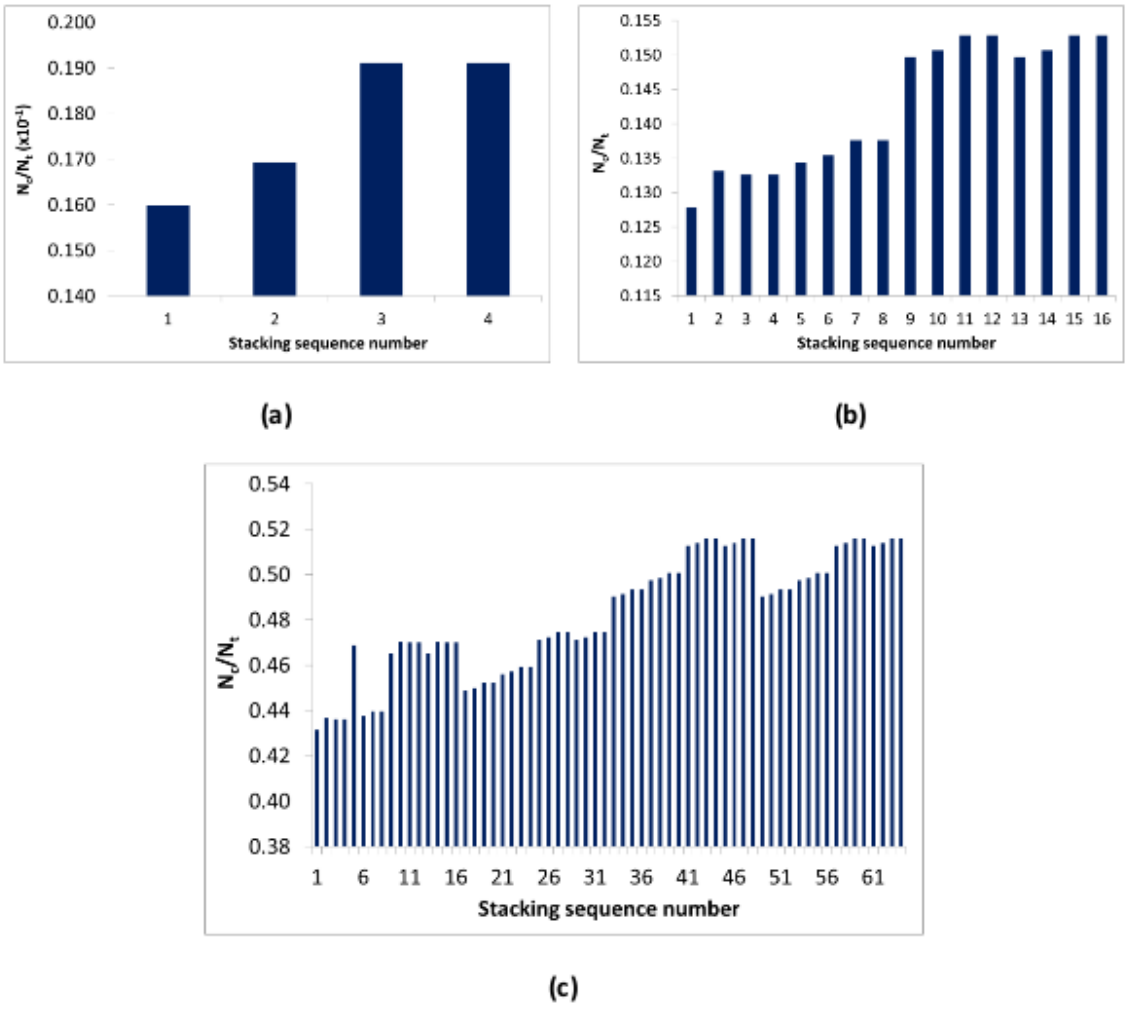

Figure 7: Ratio of N_C/N_t for all possible combinations of stacking sequence of symmetric UD laminates from 4 fibre orientation and made of (a) 2 layers, (b) 4 layers, (c) 6 layers. Set target buckling load is 200 N/mm. All failed.

Table 3: Analytical critical buckling load for all possible stacking sequences of 2, 4 and 6 layers of symmetric UD laminates when the set target buckling load is 200 N/mm.

No. of layers	Stacking no.	Sequence	Nc (N/mm)	Nc/Nt	Pass/Fail
2	1	$[0]_s$	3.20	0.016	Fail
	2	$[90]_s$	3.39	0.017	Fail
	3	$[45]_s$	3.82	0.019	Fail
	4	$[-45]_s$	3.82	0.019	Fail
4	1	$[0_2]_s$	25.56	0.128	Fail
	2	$[0/90]_s$	26.63	0.133	Fail
	3	$[0/45]_s$	26.53	0.133	Fail
	4	$[0/-45]_s$	26.53	0.133	Fail
	5	$[90/0]_s$	26.88	0.134	Fail
	6	$[90_2]_s$	27.09	0.135	Fail
	7	$[90/45]_s$	27.52	0.138	Fail
	8	$[90/-45]_s$	27.52	0.138	Fail
	9	$[45/0]_s$	29.94	0.150	Fail
	10	$[45/90]_s$	30.14	0.151	Fail
	11	$[45_2]_s$	30.58	0.153	Fail
	12	$[45/-45]_s$	30.58	0.153	Fail
	13	$[-45/0]_s$	29.94	0.150	Fail
	14	$[-45/90]_s$	30.14	0.151	Fail
	15	$[-45/45]_s$	30.58	0.153	Fail
	16	$[-45_2]_s$	30.58	0.153	Fail
6	1	$[0_3]_s$	86.27	0.431	Fail
	2	$[0_2/90]_s$	87.34	0.437	Fail
	3	$[0_2/45]_s$	87.24	0.436	Fail
	4	$[0_2/-45]_s$	87.24	0.436	Fail
	5	$[0/90/0]_s$	93.77	0.469	Fail
	6	$[0/90_2]_s$	87.52	0.438	Fail
	7	$[0/90/45]_s$	87.95	0.440	Fail
	8	$[0/90/-45]_s$	87.95	0.440	Fail
	9	$[0/45/0]_s$	93.03	0.465	Fail
	10	$[0/45/90]_s$	94.10	0.470	Fail
	11	$[0/45_2]_s$	93.99	0.470	Fail
	12	$[0/\pm 45]_s$	93.99	0.470	Fail
	13	$[0/-45/0]_s$	93.03	0.465	Fail
	14	$[0/-45/90]_s$	94.10	0.470	Fail
	15	$[0/-45/45]_s$	93.99	0.470	Fail
	16	$[0/-45_2]_s$	93.99	0.470	Fail
	17	$[90/0_2]_s$	89.78	0.449	Fail
	...	...	...	...	...
	40	$[45/90/-45]_s$	100.15	0.501	Fail
	41	$[45_2/0]_s$	102.56	0.513	Fail
	42	$[45_2/90]_s$	102.76	0.514	Fail
	...	...	...	...	...
	62	$[-45_2/0]_s$	102.76	0.514	Fail
	63	$[-45_2/45]_s$	103.20	0.516	Fail
	64	$[-45_3]_s$	103.20	0.516	Fail

Table 4: Analytical critical buckling load for all possible stacking sequences of 8 layers of symmetric UD laminates when the set target buckling load is 200 N/mm. All passed.

Stacking no.	Sequence	Nc (N/mm)	Nc/Nt	Tested specimens
1	$[0_4]_s$	204	1.0225	
2	$[0_3/90]_s$	206	1.0278	
3	$[0_3/45]_s$	205	1.0273	
4	$[0_3/-45]_s$	205	1. 0273	
5	$[0_2/90/0]_s$	212	1.0600	
6	$[0_2/90_2]_s$	213	1.0653	B3
...	...	...	...	
17	$[0/90/0_2]_s$	207	1.0373	B1
...	...	...	...	
76	$[90/0/\pm 45]_s$	216	1.0814	B2
...	...	...	...	
185	$[\pm 45/45/0]_s$	244	1.2199	
186	$[\pm 45/45/90]_s$	244	1.2209	
187	$[\pm 45/45_2]_s$	245	1.2231	
188	$[\pm 45_2]_s$	245	1.2231	B4
189	$[45/-45_2/0]_s$	244	1.2199	
190	$[45/-45_2/90]_s$	244	1.2209	
191	$[45/-45_2/45]_s$	245	1.2231	
192	$[45/-45_3]_s$	245	1.2231	
...	...	...	...	
253	$[-45_3/0]_s$	244	1.2199	
254	$[-45_3/90]_s$	244	1.2209	
255	$[-45_3/45]_s$	245	1.2231	
256	$[-45_4]_s$	245	1.2231	

Table 5: Comparison of critical buckling load from experiment, analytical (CLPT), and finite element eigen solution when the set target buckling load is 200 N/mm.

Stacking sequence	No. of layers	Specimen	Analytical N_C	Experimental N_C	FEA Eigen N_C	% deviation of N_C between analytical & experiment	% deviation of N_C between FE Eigen & experiment
$[0/90/0_2]_s$	8	B1	207	173 ± 60	208	-16.4	-16.8
$[90/0/\pm 45]_s$	8	B2	216	153 ± 20	188	-29.2	-18.6
$[0_2/90_2]_s$	8	B3	213	185 ± 5	202	-13.1	-8.4
$[\pm 45_2]_s$	8	B4	245	213 ± 10	220	-13.1	-3.2

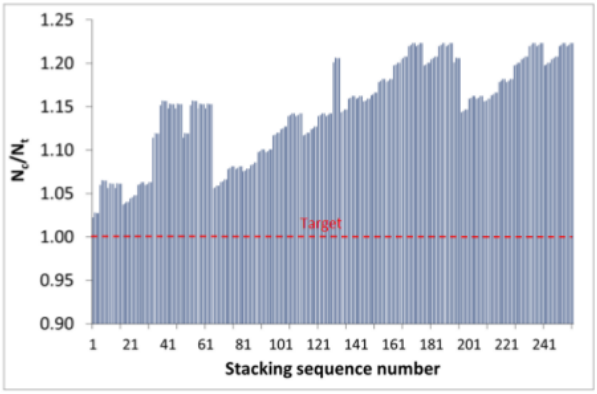

Figure 8: Ratio of N_C/N_t for all possible combinations of stacking sequence of symmetric UD laminates made of 8 layers from 4 options according to Table 3. Set target buckling load is 200 N/mm. All passed.

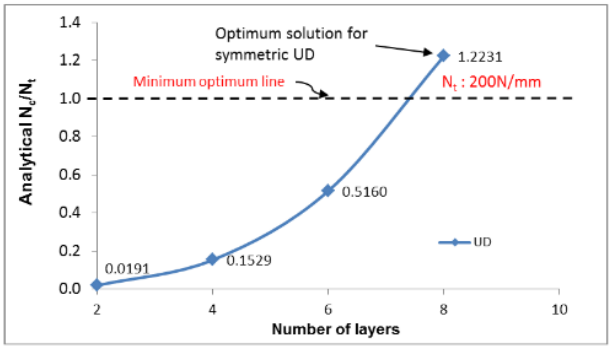

Figure 9: History of progression of critical buckling load for the fittest laminates made of UD plies as the number of plies is increased. Set target buckling load is 200 N/mm.

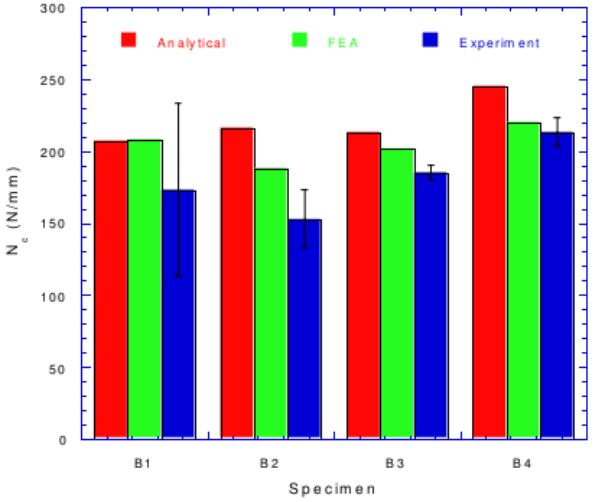

Figure 10: Comparision of critical buckling load from experiment, analytical (CLPT), and finite element eigen solution for sequences B1, B2, B3 and B4 shown in Table 4. Set target buckling load is 200 N/mm.

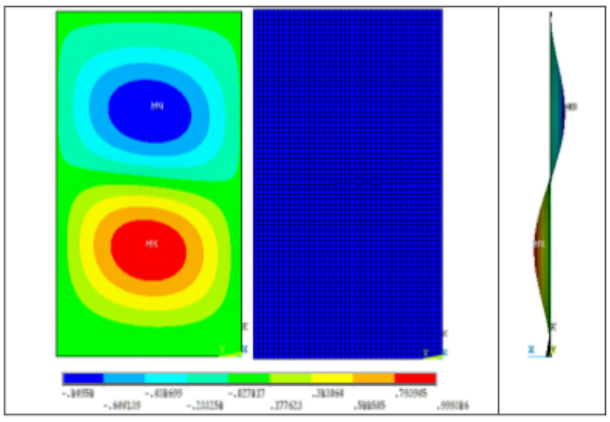

Figure 11: The first mode shape of $[\pm 45_2]_s$ laminated plate (B4 specimen); $m = 2$, $n = 1$, top view (left) and side view (right). The contour indicates ratio of w/w_{max}.

6 Conclusion

In this work, enumeration search optimisation method (ESM) and classical laminated plate theory (CLPT) were used to develop a computer programme to find the optimum stacking sequence. ESM is one of the discrete optimisation methods by which many engineering problems might be solved. The developed programme is able to find the lightest laminate that is able to withstand a set target buckling load. This is achieved by selecting the optimum stacking sequence from a set of predefined ply angles while maximizing the buckling load capability. The optimum stacking sequence is the output of the computer programme and no chart is required to find the plies angle.

In the ESM method all possible combinations of design variables, i.e. fibre orientation and number of plies, using a bottom-up approach were examined and the best combination of plies angle and number of layers was found. The optimum lay-up resulted in the laminate minimum weight and satisfied the target critical buckling load. The ESM optimisation code was written for MATLAB using CLPT for calculation of the critical buckling load.

A case study has been done and the optimum number of layers for symmetric unidirectional plies for the 200 N/mm target critical buckling load from fibre orientation of 0°, 90°, 45° and −45° was found to be eight layers with sequence $[\pm 45_2]_s$. Laminated plate specimens from the optimum (B4 specimen) and a selection of non-optimum (B1-B3 specimens) were manufactured and tested. The critical buckling load from experimental results is compared with those from the ESM and FE analysis. The percentage difference of the critical buckling load, N_C, calculated from the analytical and FEA eigen solutions,

with those from experiments are -13.1% and -3.2%, respectively. It should be noted that there are variations in the experimental buckling load from the repeat tests as maintaining the exact consistency of geometric dimensions and microstructures of the specimens is not possible.

It has been shown that the enumeration search method (ESM) is a powerful tool for finding the global optimum design at a reasonable computing cost using simple mathematical formulation. The method works very well for small to medium-size number of variables, but it very rapidly becomes unworkable for problems with many variables, e.g. for a very thick laminate with many fibre orientation angles.

Acknowledgement: Financial support by the Directorate General of Higher Education, Republic of Indonesia, for PhD study of the first author through the institution Human Resources and Development of Universitas Muhammadiyah Surakarta, Indonesia, is appreciated.

Nomenclature

a Length of plate
A Area
A_{ij} The extensional stiffness
b Width of plate
B_{ij} Coupling stiffness
D_{ij} Bending stiffness
E_{ij} Young's modulus
G_{ij} Shear modulus
$[K]$ Stiffness matrix
C $\cos\theta$
s $\sin\theta$
nl Number of layers
N_C Critical buckling load
N_t Target buckling load
N_x In-plane load in x-direction
N_y In-plane load in y-direction
N_{xy} In-plane shear load
P In-plane load
P_c Critical buckling load
p_x, p_y, p_z distributed loads (force/area)
Q_{ij} Reduced stiffness matrix
$\overline{Q_{ij}}$ Transformed reduced stiffness matrix
$[S]$ Initial stress matrix
S Shear strength
w Out-of-plane displacement
X_t Tensile strength in fibre direction.
Y_t Tensile strength in normal to fibre direction.
z_k Ply distance from mid plane
θ Ply angle
λ_i i^{th} eigenvalue
ν_{ij} Poisson's ratio
$\{\Psi_i\}$ The i^{th} eigenvector of displacements

References

[1] Satheesh R., Narayana G., Ganguli R., Conservative design optimization of laminated composite structures using genetic algorithms and multiple failure criteria, J. Compos. Mater., 2010, 44(3).
[2] Gurdal Z., Haftka R.T., Hajela P. (Eds.), Design and optimization of laminated composite materials, New York, A Wiley-Interscience Publication, John Wiley & Sons, Inc., 1999, 19–328.
[3] Kathiravan R., Ganguli R., Strength design of composite beam using gradient and particle swarm optimization, Compos. Struct., 2007, 81(4), 471–79.
[4] Gyan S., Ganguli R., Naik G.N., Damage-tolerant design optimization of laminated composite structures using dispersion of ply angles by genetic algorithm, J. Reinf. Plast. Compos., 2012, 31(12), 799–814.
[5] Kassapoglou C., Design and analysis of composite structures with applications to aerospace structures, West Sussex, John Wiley & Sons, Ltd, 2nd Edition, 2013.
[6] Fukunaga H., Sekine H., Sato M., Iino A., Buckling design of symmetrically laminated plates using lamination parameters, Comput. Struct., 1995, 57(4), 643–649.
[7] Walker M., Adali S., Verijenko V.E., Optimization of Symmetric Laminates for Maximum Buckling Load Including the Effects of Bending-Twisting Coupling, Comput. Struct., 1996, 26(1), 313–319.
[8] Walker M., Multiobjective design of laminated plates for maximum stability using the finite element method, Compos. Struct., 2001, 54, 389–93.
[9] Walker M., The effect of stiffeners on the optimal ply orientation and buckling load of rectangular laminated plates, Comput. Struct., 2002, 80, 2229–39..
[10] Sciuva D.M, Gherlone M., Lomario D., Multiconstrained optimization of laminated and sandwich plates using evolutionary algorithms and higher-order plate theories, Compos. Struct., 2003, 59, 149–54.
[11] Adali S., Lene F., Duvaut G., Chiaruttini V., Optimization of laminated composites subject to uncertain buckling loads, Compos. Struct., 2003, 62, 261–269.
[12] Kogiso N., Shao S., Murotsu Y., Reliability-based optimum design of a symmetric laminated plate subject to buckling, Struct. Optimization, 1997, 14, 184–192.
[13] Latalski J., Ply thickness tolerances in stacking sequence optimization of multilayered laminate plates, J. Theor. Appl. Mech. 2013, 51, 1039–1052.
[14] Lindgaard E., Lund E., Nonlinear buckling optimization of composite structures, Comput. Methods in Appl. Mech. Eng., 2010, 199(37-40), 2319–2330.

[15] Hemmatian H., Fereidoon A., Sadollah A., Bahreininejad A., Optimization of laminate stacking sequence for minimizing weight and cost using elitist ant system optimization, Adv. Eng. Soft., 2013, 57, 8–18.
[16] Kim D.-H., Choi D.-H., Kim H.-S., Design optimization of a carbon fiber reinforced composite automotive lower arm, Composites Part B, 2014, 58, 400–407.
[17] Ferreira R., Rodrigues H.C., Guedes J.M., Hernandes J.A., Hierarchical optimization of laminated fiber reinforced composites, Compos. Struct., 2014, 107, 246–259.
[18] Ganguli R., Optimal Design of Composite Structures: A Historical Review, J. Indian Inst. Sci., 2013, 93(4), 557–70.
[19] Waddoups M.E., Structural airframe application of advanced composite materials - analytical methods, AFML-TR-69-101, VI Air Force Materials Laboratory, Wright-Patterson Air Force Base, Ohio, 1969.
[20] Verette R.M., Stiffness, strength and stability optimization of laminated composites, NOR-70-138, Northrop Aircraft Co., Hawthorne, California, 1970.
[21] Legland D., Beaugrand J., Automated clustering of lignocellulosic fibres based on morphometric features and using clustering of variables, Ind. Crop. Prod., 2013, 45, 253–261.
[22] Park W.J., An optimal design of simple symmetric laminates under the first py failure criterion, J. Compos. Mater., 1982, 16, 341–355.
[23] Weaver P.M., Designing composite structures: Lay-up selection, In: Proceedings of The Institution of Mechanical Engineers-part G, J. Aerospace. Eng., 2002, 216, 105–116.
[24] Todman T., Fu H., Tsaoi B., Mencer O., Luk W., Smart enumeration: a systematic approach to exhaustive search, Integrate Circuit and System Design, 2009, 5349, 429–438.
[25] Nievergelt J., Exhaustive search, combinatorial optimization and enumeration: exploring the potential of raw computing power, in SOFSEM 2000, LNCS 1963, Berlin Heidelberg, Springer-Verlag, 2000, 18–35.
[26] Chang K., Markov I.L., Bertacco V., Postplacement rewiring by exhaustive search for functional symmetries, ACM Trans. Des. Autom. Electron. Syst., 2007, 32, 1–21.
[27] Chinneck J.W., Practical Optimization: a Gentle Introduction, 2010.
[28] Cornuejols G., Revival of the Gomory Cuts in the 1990s, Ann. Oper. Res., 2007, 149, 63–66.
[29] Cornuejols G., Valid Inequalities for Mixed Integer Linear Programs, Math. Program. Ser. B, 2008, 112, 3–44.
[30] Nylander H., Initially deflected thin plate with initial deflections affine to additional deflection, IABSE Publications, 1951.
[31] Falzon B.G., Stevens K.A., Davies G.O., Postbuckling Behaviour of A Blade-stiffened Composite Panel Loaded in Uniaxial Compression, Compos. Part A, 2000, 31, 459–468.
[32] Jones R.M., Mechanics of Composite Materials, Taylor & Francis, 1998.
[33] Barbero J.E., Introduction to composite materials design, 2nd Ed., CRC Press Taylor & Francis Group, 2011.
[34] Shukla K.K., Nath Y., Kreuzer E., Sateesh Kumar K.V., Buckling of laminated composite rectangular plates, J. Aerospace Eng., 2005, 18(4), 215–223.
[35] Campbell F., Structural Composite Materials, ASM Int., 2010.